UNITED NATIONS UNIVERSITY
UNU-GTP
Geothermal Training Programme

Orkustofnun, Grensasvegur 9,
IS-108 Reykjavik, Iceland

Reports 2014
Number 15

AIR QUALITY IMPACT ASSESSMENT: H_2S DISPERSION MODELLING FOR THE SABALAN GEOTHERMAL POWER PLANT, NW-IRAN

Ali Hosseinzadeh
SUNA – Renewable Energy Organization of Iran
Yadegare Emam Highway, Poonake Bakhtari Ave., Shahrake Ghods
P.O. Box 14155-6398, Tehran
IRAN
Ali_hz61@yahoo.com

ABSTRACT

In this study, the AERMOD dispersion modelling was applied to estimate the spatial distribution of H_2S concentrations in northwest Sabalan geothermal area. These estimates were made to assess the potential environmental impact of H_2S due to the exploitation of the proposed 55 MW_e Sabalan geothermal power plant. The study was done to provide recommendations concerning the local air quality and health effects in the populated areas close to the geothermal field, and for the workers in the vicinity of the proposed geothermal power plant. Two scenarios based on different locations of the power plant (emission source) were modelled, for 1, 8, and 24 hours, and 8 months averaging time, using available meteorological data from January to August, 2009. The modelling results are compared to the international ambient air quality and occupational standards. The results show that no significant health and environmental impacts are expected in northwest Sabalan geothermal area due to the proposed geothermal power plant.

1. INTRODUCTION

Compared to fossil fuels, geothermal energy is an environmentally friendly energy source for electricity generation because no combustion of fuel takes place during its production. The use of geothermal energy instead of fossil fuel effectively contributes to a reduction in CO_2 emissions. According to the EPA, the average rate of carbon dioxide emissions for coal-fired power plants and natural gas power plants is 1020 kg CO_2/MWh and 515 kg CO_2/MWh, respectively. Whereas for a geothermal power plant it is about 82 kg CO_2/MWh (Holm et al., 2012). In addition, compared to natural gas-fuelled electrical power plants, geothermal power plants produce no nitrous oxide. Nevertheless, as with any other source of energy, production of electricity derived from geothermal energy also causes environmental pollution, although on a much smaller scale (Gupta and Roy, 2007). One of the highlighted environmental issues in utilising geothermal systems is the discharge of non-condensable gases (NCG) to the atmosphere. The NCG present in geothermal fluid are a mixture of CO_2, H_2S, H_2, Hg, NH_3 and CH_4. Among all the NCG emitted, H_2S is of the greatest environmental concern, not only because of its noxious smell in low concentrations, but also due to its toxicity and health impacts at high concentrations (Kristmannsdóttir et al., 2000).

The commissioning of a 55 MW_e power plant in the Sabalan geothermal field certainly means a big step for geothermal development in Iran. However, the impacts associated with a geothermal development project may include negative effects on local air quality. Therefore, an assessment of the impacts of the proposed power plant on air quality is an integral part of the environmental assessment of this project. One way to study the air pollution is to use models that can predict the spatial distribution, and concentration of the pollutant with time (Nyagah, 2006).

Modelling air pollution is an important tool in devising strategies to manage the air pollution (Ólafsdóttir et al., 2014). Air quality models attempt to simulate the physical and chemical processes in the atmosphere; those may involve transport, dispersion, deposition and chemical reactions, to estimate pollutant concentrations at a downwind receptor location (Hung, 2010).

There are five general types of air dispersion models: Box model, Gaussian model, Lagrangian model, Eulerian model, and Computational Fluid Dynamics (CFD) model. The Gaussian model is the most commonly used model type. It assumes that the air pollutant dispersion has a Gaussian distribution and is normally used for predicting the dispersion of continuous, buoyant air pollution plumes originating from ground-level or elevated sources. Gaussian models may also be used for predicting the dispersion of non-continuous air pollution plumes. Examples of Gaussian models are: OSPM, UBM, CALINE4, UK-ADMS, and AERMOD (Holmes and Morawska, 2006).

AERMOD, the recommended model by the US EPA, has been used to model the distribution of various air pollutants including Hg, SO_2, NO_x, PM_{10} and H_2S. AERMOD uses a Gaussian and a bi-Gaussian approach in its dispersion models. It can calculate from hourly to the annual concentrations average of pollutants in ambient air. The model handles a variety of pollutant sources in a wide variety of settings such as rural and urban as well as flat or complex terrain (Kumar et al., 2004).

The aim of this report is to use dispersion modelling for assessment of the temporal and spatial distribution of H_2S in the generation site and populated areas close to the planned 55MW_eSabalan geothermal power plant. The predicted H_2S ground level concentrations will be compared to the international ambient air quality guidelines and occupational safety standards.

2. HYDROGEN SULPHIDE

Sources of H_2S are both natural and anthropogenic. It is released from volcanoes, sulphur springs, undersea vents, swamps, salt marshes, and stagnant bodies of water, and is found in association with crude petroleum and natural gas. Hydrogen sulphide is also associated with municipal sewers and sewage treatment plants, landfill gases, manure handling operations, pulp and paper operations, and geothermal power plants (EOHP, 2006).

2.1 Physical and chemical properties

Hydrogen sulphide (H_2S) is a flammable, colourless gas at ambient temperature and pressure with a characteristic odour of rotten eggs (Table 1). The levels of hydrogen sulphide in the air are typically low. The amount of hydrogen sulphide naturally found in the air has been estimated at 0.11-0.33 ppb (0.15-0.46$\mu g/m^3$). Lower levels (0.02-0.07 ppb; 0.03-0.1 $\mu g/m^3$) have been observed in some remote areas (EOHP, 2006).

Hydrogen sulphide does not absorb the solar radiation reaching the troposphere and, thus, is photo-chemically stable. The atmospheric lifetime of H_2S is affected by ambient temperature and other ambient conditions including humidity, sunlight, and the presence of other pollutants. Decreased temperatures

and sunlight, as well as lower levels of hydroxide radicals in northern regions during winter, increase the atmospheric residence time of H_2S (Idriss et al., 2004).

TABLE 1: The physicochemical properties of H_2S (SCOEL, 2007)

Properties	Description
Empirical formula	H_2S
Molecular weight	34.08 g/mol
Freezing point at 101.3 kPa	-85.5ºC
Boiling point at 101.3 kPa	-60.7ºC
State at room temperature	Gas
Vapour pressure at 25.5ºC	2026 kPa
Vapour density (air=1)	1.19
Flammability	Extremely flammable
Explosive limits in air (vol/vol)	Lower limit:4.3% , Upper limit: 45.5%
Solubility(w/w) in water at 20 ºC	0.4%
Odour	Strong odour of rotten eggs

After emission into the air, H_2S is dispersed and eventually removed. Resident time in the atmosphere ranges from about one day to more than 40 days, depending upon season, latitude, and atmospheric conditions.

H_2S released to the atmosphere is oxidized in reactions with $OH^{\bullet}$ radicals. The probable mechanism of this hydrogen absorption reaction is as follows:

$$H_2S + OH^{\bullet} = H_2O + SH^{\bullet}$$

With the reaction rate constant $k_{298} = (4.5 \pm 1.0)\ 10^{-12}$ cm^3molecule/sec.

Dependency of the rate constant (K) on temperature (T) follows the Arrhenius equation:

$$K = A\ e^{-E/RT}$$

where A, E and R are the Arrhenius constant (frequency factor), activation energy and universal gas constants, respectively.

The $SH^{\bullet}$ radical is oxidized to a transient molecule HSO_3, and then to sulphuric acid (H_2SO_4) as a final product. Other parallel reactions of H_2S with other oxidants such as NO_2, O_2 and O_3 are not important, being much slower than the oxidation with $OH^{\bullet}$ radicals (Idriss et al., 2004).

2.2 Health and environmental impacts

Human health effects of exposure to hydrogen sulphide, an irritant and asphyxiate, depend on the concentration of the gas, the length of exposure, the state of health, and age and level of activity of the person exposed. Observations of effects on people exposed to different concentrations of H_2S in the air indicate that there is a progression in the severity of adverse health effects. Because of the sensitivity of the olfactory nerves, it is possible for the human to detect the presence of H_2S in the air at a concentration of < 0.14 mg /m^3. The odour is very offensive at 4.2 - 7 mg/m^3 and, at a concentration of 210 mg /m^3, the olfactory nerves are unable to detect the odour, presumably because of olfactory nerve damage or sensory overload. A dose dependent progression of adverse effects starts with eye irritation at 14 - 28 mg/m^3 and ending with collapse and death at 1400 - 2800 mg/m^3 (MESB, 2000).

Because hydrogen sulphide is a gas, inhalation is the major route of exposure to hydrogen sulphide. Inhalation exposure to hydrogen sulphide causes health effects in many systems. Health effects that have been observed in humans due to exposure to hydrogen sulphide include ocular, neurological, cardiovascular, metabolic, respiratory, reproductive effects and death. Respiratory, neurological, and ocular effects are the most sensitive end-points in humans. There are no adequate data on carcinogenicity (WHO, 2003).

Most human data are derived from acute poisoning case reports, occupational exposures, and limited community studies (WHO, 2003). According to the U.S. Occupational Safety and Health Administration records, there were 80 fatalities in 57 H_2S incidents from 1984 to 1994 (Fuller and Suruda, 2000).

Hydrogen sulphide is found in nearly all high-temperature (T > 150°C) geothermal fluids. It is probably formed by one or more of the following mechanisms: reaction of sulphur that is present in reservoir rocks with hot water, magmatic exhalation, or thermal metamorphism of marine sedimentary rocks (Wahl, 1977).Some studies in geothermal active areas have indicated that chronic exposure to H_2S increases nervous system diseases and cardiovascular diseases, as well as respiratory diseases (Bates et al., 2002; Durand and Wilson, 2006).

Several studies have shown that exposure to H_2S at low levels can increase plant growth and/or the rate of physiological processes in a variety of species. Positive growth and physiological responses to pollutant exposure has sometimes been termed as a "fertilizer" effect. However, the increment of plant photosynthetic rates in the absence of corresponding enhanced dry weight accumulations can be a stress response to a toxic compound. Plants may increase their rate of photosynthesis in order to keep up with the required rate of injury compensation and repair. Once plants are unable to keep up with the required rate of repair, detectable reductions in plant dry weight accumulation may occur (Khalil et al., 1996; De Kok et al., 1997).

2.3 Ambient air quality standards for hydrogen sulphide

There are no ambient air quality standards for H_2S environmental concentrations in Iran. Criteria pollutants (NO_2, SO_2, CO, HC(NMHC) and SPM (Suspended Particulate Matter) are the pollutants involved in air quality assessment in Iran. Therefore, WHO guidelines and standards (WHO, 2000) have been adopted in Iran. The standards for H_2S vary between countries, although many use the WHO recommendations (Table 2).

TABLE 2: Various ambient air quality standards for H_2S

Country/Agency	Relevant Law	Value (µg/m3)[a]	Averaging period
WHO	Air Quality Guidelines 2nd Edition, 2000	150 7	24 hours 30 minutes
Iceland	Regulation 514/2010, Annex1	50	24 hours
New Zealand	Ambient Air Quality Guidelines, 2002	7	1 hour
State of California, USA	State Ambient Air Quality Standards, Cal EPA 2005	42	1 hour
State of New York, USA	State Ambient air quality standard, DEC 2005	14	1 hour
State of New Mexico, USA	State Ambient air quality standard	14	1 hour
State of Arizona, USA	State Ambient air quality standard,(AAAQGs) 1999	180	1 hour
Europe	Air Quality Guidelines for Europe, 2000	150 7	24 hours 30 minutes
Germany	Odour Threshold Values for Ambient Air Quality Protection, FEA, 2004	3	-
Korea	Atmospheric and Environmental Protection Laws(Chap. 3 Sec.30)	84[b] 28[c]	- -

[a]The conversion factors for hydrogen sulphide in air (25°C, 101.3 kPa) are 1 mg/m^3= 0.717 ppm, 1 ppm = 1.394 mg/m^3. [b]In industrial areas. [c]In residential areas

2.4 Occupational health guidelines for hydrogen sulphide

People who work in certain industries can be exposed to high levels of hydrogen sulphide. These industries include rayon textiles manufacturing, pulp and paper mills, petroleum and natural gas drilling operations, wastewater treatment plants, geothermal power plants, smelting and mining. The occupational exposure standards provide threshold limits for chemical substances in the working environment based on the health effects safety guidelines (Aráuz, 2014). At present, there is no regulation for the occupational exposure limits for hydrogen sulphide in Iran. Hence, ACGIH, OSHA and NIOSH guidelines have been adopted in Iran. The occupational exposure limits for H_2S vary between different institutes and countries (Table 3).

TABLE 3: International occupational exposure limits for H_2S

Country	Level (ppm)	Level µg/ m^3	Averaging Period	Guideline Type	Date of Implementation	Relevant Law	Ref.
UK	10	14000	15 min	[1]MEL		New	a
	5	7000	8 hours[2]TWA	MEL		New	a
USA	20		8 hours TWA	[3]PEL-C		OSHA Regulations (Standards 29 CFR)	b
	10	14000	10 min ceiling	[4]REL-C	2003	NIOSH	c
	0.1		1 hour	[5]ERPG-1	2003	Emergency Response Planning Guideline	d
	30		1 hour	[6]ERPG-2	2003	Emergency Response Planning Guideline	d
	100		1 hour	[7]ERPG-3	2003	Emergency Response Planning Guideline	d
	10	14000	8 hours	[8]TLV-TWA	2009	ACGIH	e
	15	21000	15 min	TLV-[9]STEL			

a.HSE, 2002. Occupational Exposure Limits 2002. HSE Books, Sudbury.

[1]Maximum Exposure Limits

b. OSHA 2006 29CFR1910.1000, Table Z-2

[2]Time-Weighted Average (TWA): time-weighted average concentration for a conventional 8-hour workday and a 40-hour workweek, to which it is believed that nearly all workers may be repeatedly exposed, day after day, without adverse effect.

[3]Permissible Exposure Limit (PEL-C): regulatory limit (ceiling) on the amount or concentration of a substance in the air, and they are enforceable.

c.NIOSH Pocket Guide to Chemical Hazards (NPG).http://www.cdc.gov/niosh/npg/npg.html

[4]Recommended Exposure Levels (REL-C): refers to the concentration that should not be exceeded during any part of the working exposure (ceiling).

d.AIHA Emergency Response Planning Guidelines Committee, 2004. 2004 Emergency Response Planning Guidelines (ERPG) Update Set, American Industrial Hygiene Association, Fairfax.

[5]ERPG–1: The maximum airborne concentration below which it is believed nearly all individuals could be exposed for up to 1 hour without experiencing more than mild, transient adverse health effects or without perceiving a clearly defined objectionable odour.

[6]ERPG–2: The maximum airborne concentration below which it is believed nearly all individuals could be exposed for up to 1 hour without experiencing or developing irreversible or other serious health effects or symptoms that could impair an individual's ability to take protective action.

[7]ERPG–3: The maximum airborne concentration below which it is believed individuals could be exposed for up to 1 hour without experiencing or developing life-threatening health effects.

e. https://www.acgih.org/about/committees/c_tlvpa.htm

[8]Threshold Limit Value (TLV): exposure limits "to which it is believed nearly all workers can be exposed day after day for a working lifetime without ill effect".

[9]Short Term Exposure Limit (STEL): the concentration to which it is believed that workers can be exposed continuously for a short period of time without suffering from irritation, chronic or irreversible tissue damage, or narcosis.

3. NORTHWEST SABALAN GEOTHERMAL FIELD

3.1 History of geothermal development in NW-Sabalan

Interest in geothermal energy originated in Iran when James R. McNitt, a United Nations geothermal expert, visited the country in December 1974. In 1975, a contract among the Ministry of Energy, ENEL (Entes Nazionale per LEnergia Elettrica) of Italy and TB (Tehran Berkeley) of Iran was signed for geothermal exploration in the northwest part of Iran (Renewable Energy Organization of Iran, 2014).

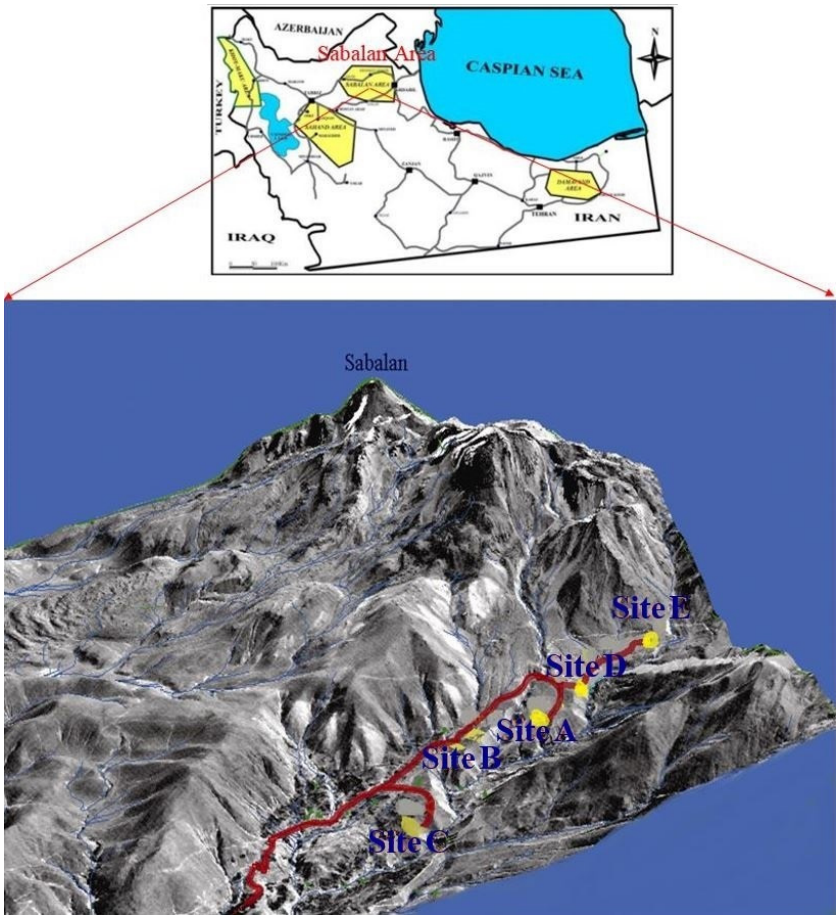

FIGURE 1: Location of northwest Sabalan geothermal field

In 1983, the result of investigations defined Sabalan, Damavand, Khoy-Maku and Sahand regions as four prospective geothermal sites in northwest Iran. AS a result of further investigation in the 1990s, following a long gap, the northwest Sabalan geothermal area was proposed as a first priority of the geothermal potential regions for detailed exploration (Renewable Energy Organization of Iran, 2014). This field lies on the northwest flank of a large strato-volcano named Mt. Sabalan, within the province of Ardabil in northwest Iran (Figure 1).

From 1998 to 2005, detailed exploration studies were conducted by SUNA of Iran and Sinclair Knight Merz Ltd (SKM) of New Zealand in two stages. The first one included geological, geochemical and geophysical surveys, and the second one the drilling of three deep exploration wells and two shallow injection wells. According to the results of geo-based surveys and well testing, NW-Sabalan geothermal field was identified as a potential reservoir for power generation purposes. Numerical modelling of the reservoir was also performed from 2004 to 2005 and the capacity of the field was estimated at being able to sustain 55 MW of power production (SKM, 2005a).

The next stage of the NW-Sabalan geothermal field development began in 2007. At that time, the EDC (Energy Development Corporation) technical team of the Philippines reviewed all the available data from NW-Sabalan. A new MT survey, re-sampling and re-evaluation of all thermal springs in the area, detailed geological mapping and remote sensing and a new discharge test of Wells NWS-1 and NWS-4 were the activities proposed and conducted prior to any future drilling in order to determine the centre of the geothermal system (EDC, 2007).

According to the results of detailed geophysical and geological investigations, the drilling and testing program for the delineation phase was carried out between May 2008 and December 2012. During this phase, six new exploratory wells (NWS-6D ,NWS-7D, NWS-8D, NWS-9D, NWS-10D and NWS-11RD) were drilled and one existing well (NWS-5D)was deepened. In addition, well logging and discharge testing were accomplished

for five production wells (NWS-5D, NWS-6D, NWS-7D, NWS-9D and NWS-10D). The results of discharge well testing revealed that the total capacity of these five wells and the previous two wells is 31 MW of electricity and 72 MW of thermal power. Furthermore, the characteristics of the Sabalan reservoir were being precisely assessed using well logging and discharge tests on the production wells (Kosari, 2011). At present, the tender for a5 MW portable power plant is in progress. Hence, the construction of the first geothermal power plant in Iran is to be completed in 2016-17; if the contractor is selected in 2014.

3.2 Characteristics of the northwest Sabalan geothermal field

3.2.1 Project area

The northwest Sabalan geothermal field is located in zone 38 of the UTM coordinate system, between 733500E - 745000E and 4232500N - 4243500N in the Moil valley on the western slopes of Mt. Sabalan Mountain. The geothermal project site is approximately 2 km southeast of Moil village, with 1,600 inhabitants, and about 16 km south of Meshkinshahr city, with 160 thousand residents. Two other villages are found to the northwest of the area, Valezir, with a population of approximately250 inhabitants, and Dizo, with 90 inhabitants.

Sparse subsistence farming and small-scale livestock activity predominates in the area. Agricultural activities and cattle farming modify a large part of the vegetation near the project area. A substantial part of the area is pastureland. The region is considered an ecologically sensitive area with a large number of springs and touristic resorts. The cold and hot springs, beautiful and unique landscapes, hiking trails, vast plains, national monuments and favourable weather conditions are all part of the natural characteristics of the project area (Porkhial, 2010). Access to the area is provided by an asphalt road from Meshkinshahr city to the village of Moil and then by gravel road to the project site. Moreover, Khiyavchai River is the major drinking water resource for Meshkinshahr residents and agricultural activities run along the site.

3.2.2 Geological settings

Tectonically, Sabalan volcano lies on the south Caspian plate, which underlies the Eurasian plate to the north and overlies the Iranian plate, producing northwestwardly compression (McKenzie, 1972).Mt. Sabalan is located in a Quaternary (Pleistocene-Pliocene) andesitic volcanic complex that covers an area of approximately 2500km^{2}and NW Sabalan geothermal field is part of this area. Volcanic deposits of Sabalan volcano are characterized by altered andesitic, dacitic and trachydacitic lavas, pyroclastics, lahars, tuffs and domes that date from 0.2 – 1.3 Ma, using the K-Ar dating method (TBCE, 1979).

The project area is located within the Moil Valley, which, on satellite and aerial photographic imagery, can be seen to be a major structural zone. The stratigraphy of the Moil valley, where the deep exploration wells are located, can be divided into four major rock formations (SKM, 2005a) (Figure 2):

1. Dizu Formation - Quaternary alluvium, fan and terrace deposits.

2. Kasra Formation - Pleistocene post-caldera trachyandesitic flows, domes and lahars.

3. Taos Formation - Pleistocene syn-caldera trachydacitic to trachyandesitic domes, flows and lahars.

4. Valhazir Formation - Pliocene pre-caldera trachyandesitic lavas, tuffs and pyroclastics.

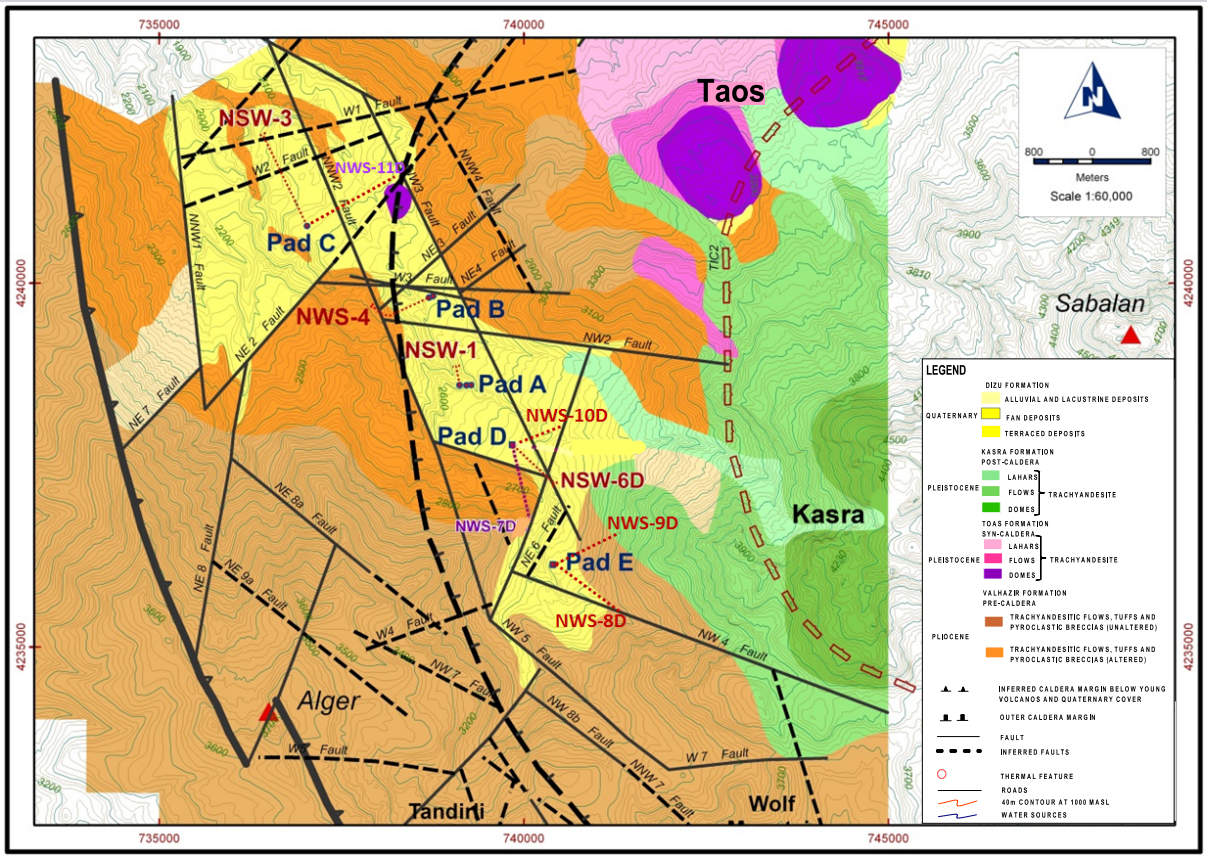

FIGURE 2: Geology of the NW Sabalan geothermal field (modified from Bogie et al., 2000)

Faridi (2010) mapped the structure of the Sabalan volcano and concluded that it is deformed in an active tectonic regime. This deformation has led to the elongation of the Sabalan caldera parallel to the regional $\sigma_3$axis. It was concluded that the Sabalan caldera is associated with an extensive hydrothermal system and fracturing in the inner and outer calderas causing the thermal source fluids to readily ascend to the surface (Kosari, 2011).

3.2.3 Geochemistry

The occurrence of chloride springs in NW Sabalan is significant since these springs indicate the presence of deep, mineralized fluids, at depth. As a rule, geothermometric calculations are done only for chloride springs; hence, temperature estimates given by other thermal waters are insignificant and should be disregarded. Low silica and cation geothermometer temperatures (~150-200°C), estimated from Gheynarde and Khosrowsu chloride springs, are expected to be mainly due to the dilute and mixed nature of these surface features. On the other hand, the presence of acid-sulphate warm springs in NW Sabalan suggests near-surface boiling in the area. Since there are no gas manifestations such as sulfatases, steaming grounds, gas vents or extensive acid-altered grounds, the extent of near-surface boiling may be localized (EDC, 2007).

The results of exploration drilling in the Moil Valley in NW Sabalan confirmed the presence of a liquid-dominated reservoir with outflows of steam and water to surface thermal areas with temperatures ranging from 225 to 240°C.

Geochemical analysis of fluid samples collected during discharge testing of 7 production wells (NWS-1, NWS-4, NWS-6D, NWS-7D, NWS-5D, NWS-9D and NWS-10D) indicates that the liquids discharged from the wells can be classified as a slightly alkaline, medium salinity, sodium-chloride waters. Quartz geothermometer yields estimates of a reservoir temperature between (230-245°C); on the

other hand, the cation geothermometer yielded estimates of a reservoir temperature higher than 260°C. This may be an indication that the deep geothermal fluid in NW Sabalan is fully equilibrated, and the highest reservoir temperature that can be expected is that given by the cation thermometer (~260°C) (EDC, 2007). The scaling potential assessment of the fluid in the wells indicates that all the wells have a high potential to form calcite scales; silica scaling is not expected to occur in the wells.

The composition of the gas dissolved in the deep liquid is represented by 98-99% in weight of CO_2 and 1-2% of H_2S and N_2. He, Ar, H_2 and CH_4 are all at very low proportions (Amistoso et al., 2013; SKM, 2004 and 2005b).

4. H_2S EMISSIONS FROM SABALAN GEOTHERMAL POWER PLANT

4.1 Concentration of H_2S in steam

According to discharge testing of the NW-Sabalan geothermal wells, the weight percent of non-condensable gases (NCG) in the steam phase is calculated to be about 2-3%, based on a steam mass percentage of about 20%.

The concentration of H_2S in steam in each well is different and varies from 83 ppm to 256 ppm (Amistoso et al., 2013; SKM, 2004, 2005b).Given that the production capacity of each geothermal well is approximately 5 MWe, the average concentration of H_2S is about 170 ppm.

4.2 Sabalan geothermal power plant

The long-term target capacity of electrical power generation in the NW-Sabalan geothermal project is expected to be 55 MWe. The proposed Sabalan geothermal power plant, in accordance with the initial design, consists of a 5 MWe pilot unit and two 25 MWe single flash units. At present, the renewable energy organization of Iran (SUNA) is in the process of constructing five MWe pilot units in the field that is expected to be commissioned in 2016-2017 as the first Iranian geothermal power plant.

The term ‘single flash power plant’ refers to an energy conversion process in which a pressurized geothermal fluid is flashed to produce a mixture of steam and liquid. After that, phases are isolated using a steam separator and the steam is sent to a turbine to drive an electric generator and produce energy. The steam exhaust from the turbine is passed through a condenser, which produces a condensate stream and non-condensable gases (Millachine, 2011). The non-condensable gases (including H_2S) are vented out of the condensers to the atmosphere in the cooling towers to enhance dispersion (Aráuz, 2014).In this way, approximately 97% of H_2S, along with other non-condensable gases (NCG), is discharged to the atmosphere and the rest of the NCG is released from a silencer, steam traps and the collection area (Franco, 2010). A simplified representation of the condensing cycle of a single flash geothermal power plant is shown in Figure 3 (Kagel, 2008).

Based on the Sabalan reservoir steam specifications and the engineering equation solver (EES) program, the steam consumption is calculated to be 2.3 kg/s per MWe, assuming that the steam enters the turbine at approximately 151°C and at 5 bar and exits the turbine at 0.1 bar pressure and 46°C saturation temperature (Radmehr, 2005). Hence, the flow rate of steam that is required for the 55 MWe Sabalan geothermal power plant is about 127 kg/s, or approximately 450 ton/h. As aforementioned, the concentration of H_2S in the steam is estimated at about 170 ppm. According to the total flow rate of the steam, the emission of H_2S from Sabalan geothermal power plant is appraised at about 21.6 g/s or 77.7 kg/h.

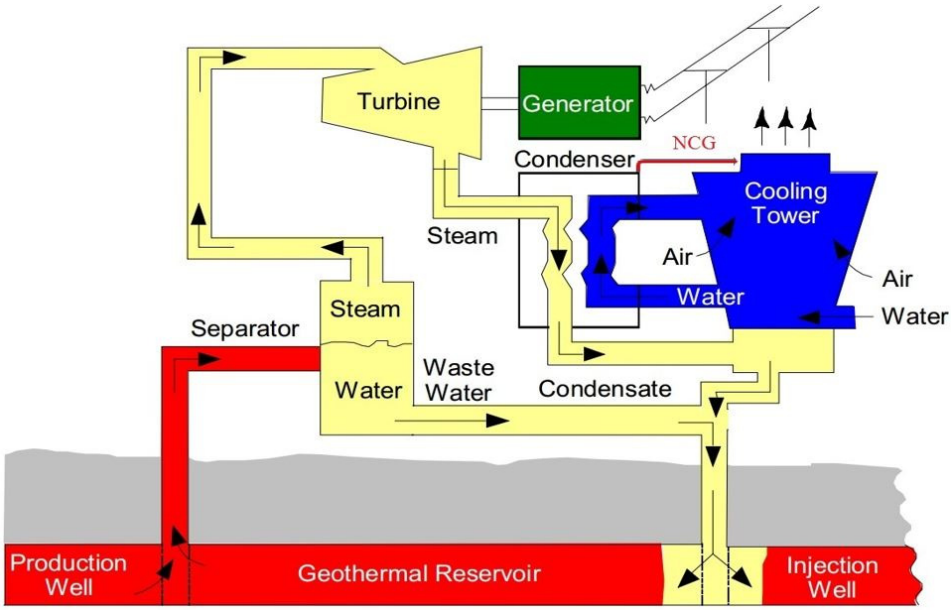

FIGURE 3: Simplified schematic of the condensing cycle at the proposed Sabalan geothermal power plant

5. DISPERSION MODELLING

Dispersion modelling uses mathematical equations to describe the atmosphere, dispersion, chemical and physical processes influencing a pollutant released from sources of a given geometry to calculate concentrations at various receptors (Holmes and Morawska, 2006). Dispersion models can provide concentration, or deposition, estimates over an almost unlimited grid of user-specified locations, and can be used to evaluate different emission scenarios. In this capacity, air dispersion modelling is a useful tool in assessing the air quality impacts associated with existing or proposed emission sources. The results of the dispersion modelling analysis can be used to develop control strategies that should ensure compliance with assessment criteria (DEC, 2005).

The models require information on the source, or sources, including pollutant emission rates, and meteorological data. In addition, they also need information on the topography of the study area (Figure 4). The models then use this information to simulate mathematically the pollutant's transport and dispersion. The output is air pollutant concentrations, for a particular time period, usually at specific receptor locations (Vallero, 2008).

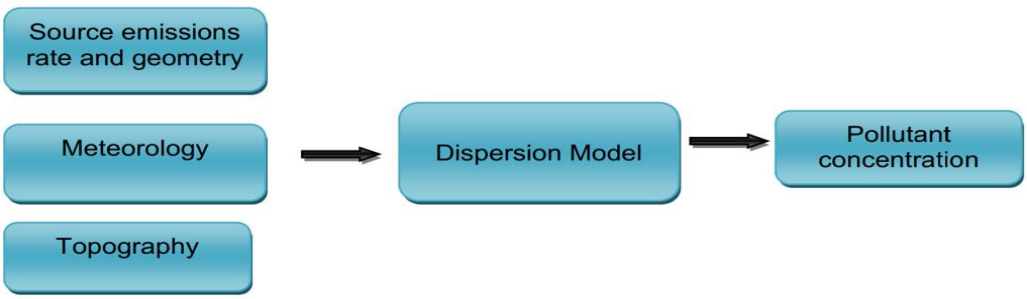

FIGURE 4: A schematic representation of the input-output of an air dispersion model (Neshuku, 2012)

5.1 Gaussian plume dispersion model

This type of model assumes that the pollutant disperses according to the normal statistical distribution (Holmes and Morawska, 2006). At the point of release, the pollutant concentration is at maximum and decreases in both lateral and vertical directions following normal distribution. The most general form of the Gaussian dispersion equation that is used for point source emissions is (Macdonald, 2003):

$$C(x,y,z;H) = \frac{\mathrm{Q}}{2\pi U_s \sigma_y \sigma_z} exp\left[-\frac{y^2}{2\sigma_y^2}\right]\left[exp\left\{-\frac{(z-H)^2}{2\sigma_z^2}\right\} + exp\left\{-\frac{(z+H)^2}{2\sigma_z^2}\right\}\right], \qquad (1)$$

where C = steady-state concentration at a point (x, y, z), µg/m^3;
Q = pollutant emission rate, µg/s;
U_s = mean wind speed at release height;
σ_y, σ_z standard deviation of lateral and vertical spread parameters, n;
y = horizontal distance from plume centreline, m;
x = downwind distance from plume source, m;
H = effective stack height (H = h +Δh) where h = physical stack height and Δh = plume rise;
z = vertical distance from ground level, m.

The first and second exponential terms represent the lateral and vertical dispersions, respectively. The Gaussian distribution determines the size of the plume downwind from the source (Figure 5). The plume size is dependent on the stability of the atmosphere and the dispersion of the plume in the horizontal and vertical directions. These horizontal and vertical dispersion coefficients (σ_y and σ_z respectively) are merely the standard deviation from normal on the Gaussian distribution curve in the y and z directions. The dispersion coefficients are functions of wind speed, cloud cover, and surface heating by the sun. The Gaussian distribution requires that the material in the plume be maintained. In other words, the plume edge must be allowed to reflect from the ground without losing any pollution. In addition, the Gaussian distribution and plume rise depend on the ground being relatively flat along the path of the plume. The topography affects atmospheric wind flow and stability; therefore, uneven terrain caused by hills, valleys, and mountains will affect the dispersion of the plume so that the Gaussian distribution must be modified (EPA, 2006).

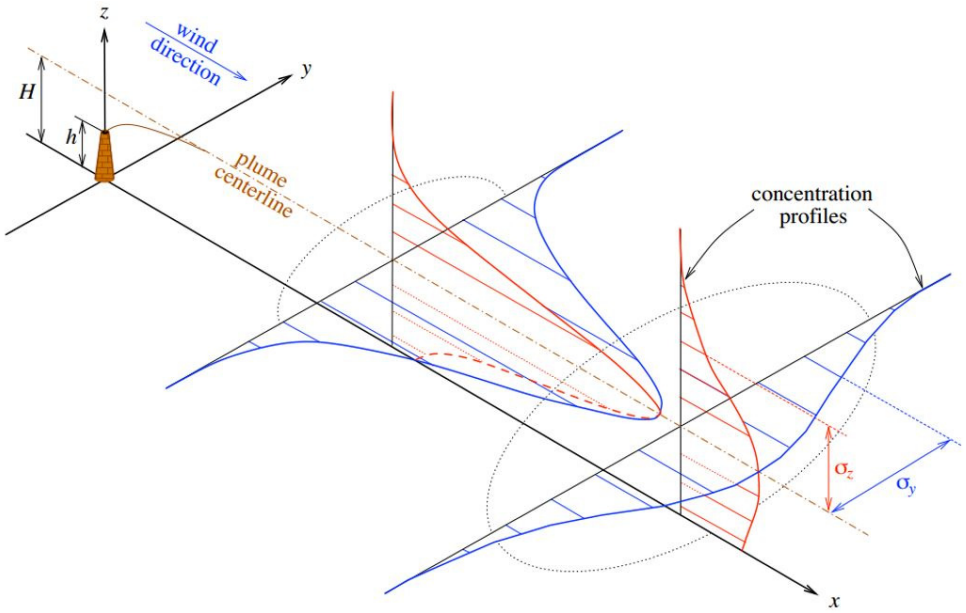

FIGURE 5: Graphical representation of double Gaussian distribution in the plume (Stockie, 2011)

5.2 AERMOD dispersion model

There is a large body of literature addressing the application of different atmospheric dispersion models and the use of these models for different situations, the evaluation of the sensitivity and uncertainty of modelling pollutant dispersion, human exposure risk assessment, as well as the usefulness of these models for epidemiological applications (Zouet al., 2010).

Dispersion software programs based on the Gaussian plume equation are widely applied to estimate the dispersions of various pollutants. AERMOD (AMS/US EPA) is a near field (less than 50 km) steady state Gaussian plume model based on planetary boundary layer (PBL) turbulence structure and scaling concepts, including treatment of both surface and elevated sources over both simple and complex terrain. It is applicable to rural and urban areas, and multiple sources including point, area, and volume sources (Vora, 2010). The model has the capacity to employ hourly sequential pre-processed meteorological data to estimate concentrations of pollutants at receptor locations at different time scales ranging from 1 h to 12 months. AERMOD can incorporate various complex algorithms and concepts. It is applied to evaluate the dispersion of a number of pollutants, including PM_{10}, hydrogen cyanide (HCN), SO_2, sulphur hexafluoride (SF_6), VOCs, NO_2 and H_2S (Seangkiatiyuth, 2011).

The AERMOD modelling system comprises a meteorological pre-processor (AERMET), a terrain pre-processor (AERMAP) and the dispersion model (AERMOD) (Figure 6).

The major purpose of AERMET is to calculate boundary layer parameters to be used by AERMOD. The AERMET requires standard meteorological observations such as wind speed, wind direction, temperature and cloud cover. It also needs the surface characteristic parameters of albedo, surface roughness and the Bowen ratio (Neshuku, 2012). It then makes use of this data for the calculations of the planetary boundary layer (PBL) parameters such as: Mixing height (z), Monin – Obukhov length (L), temperature scale, convective velocity scale (w) and surface heat flux (H) (Cimorelli et al., 2004).

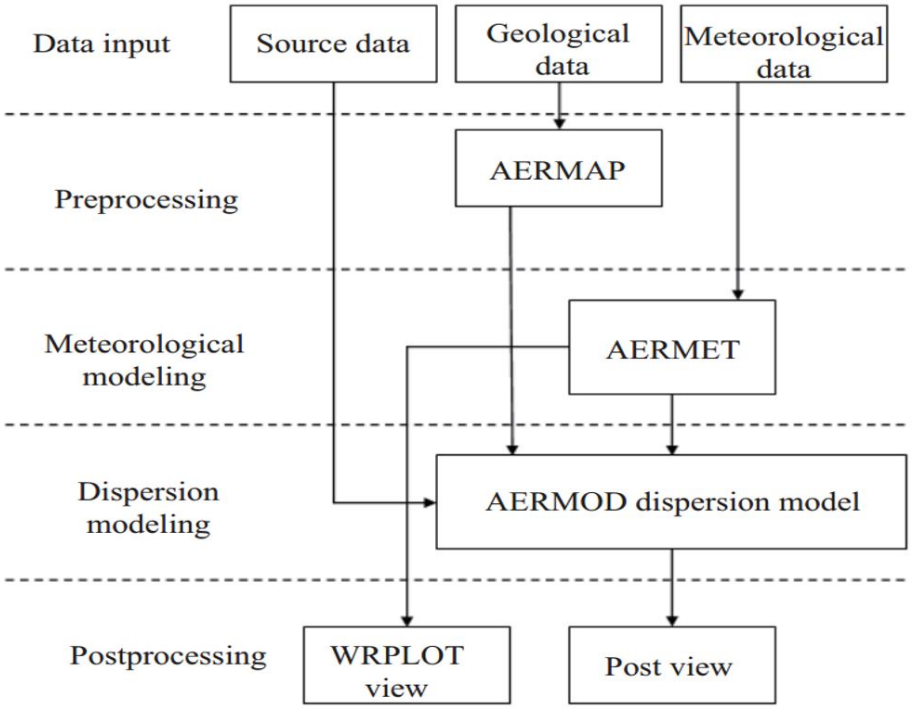

FIGURE 6: Data flow in the AERMOD modelling
(Seangkiatiyuth, 2011)

The meteorological interface, internal to AERMOD, uses these parameters to generate profiles of the needed meteorological variables, such as lateral and vertical turbulent fluctuations (v, w), vertical profiles of wind speed (u) and potential temperature gradient ($d\theta/dz$).

The second module, AERMAP is used to calculate the terrain height scale (h_c) for each receptor location, which is used to calculate the dividing streamline height. AERMAP also generates receptor grids for AERMOD. The input to AERMAP is the topographical data in a format of Digital Elevation Mapping (DEM) files. The information generated from AERMAP is then passed on to AERMOD as the location of receptors, the receptor's height above mean sea level and the receptor specific terrain height scale (h_c) (Cimorelli et al., 2004). AERMOD then uses this information from the two pre-processors to compute concentrations of pollutants, taking into account the changes in the dispersion rate with height and making use of non-Gaussian plumes in convective conditions (Perry et al., 2005).

5.2.1 Input data

Source data
According to the primary design of Sabalan geothermal power plant, it is assumed that H_2S and other NCG are vented to the atmosphere through cooling towers. Given that there is no geothermal power plant in NW Sabalan field yet, the source input model is based on the accessible data from a part of Nesjavellir geothermal power plant with similar power capacity (60 MW) (Ólafsdóttir et al., 2014) and Sabalan reservoir steam specifications. In addition, according to the proposed locations for the geothermal power plant (GPP) in northwest Sabalan geothermal project, the following scenarios are identified for H_2S dispersion modelling in the study area:

- Scenario1: it is assumed that the emission source of the Sabalan geothermal power plant (GPP) station is located at site D at 739793 mE and 4237851 mN in zone 38 of the UTM coordinate system.
- Scenario2: it is assumed that the emission source of the Sabalan geothermal power plant (GPP) station is located at site B at738715 mE and 4239776 mN in zone 38 of UTM coordinate system.

The source input model (Table 4) assumes full load operation capacity for a whole year without considering yearly maintenance or overhaul.

TABLE 4: Source input data.

Source	Capacity (MW)	Coordinate (UTM)		Base elevation (m.a.s.l.)	Stack height (m)	Stack inside diameter (m)	Gas exit temperature (ºC)	Gas exit velocity (m/s)	Emission rate (g/s)
		x	y						
GPP-Site_D (Scenario1)	55	739793	4237851	2747	13	17.8	46	9.6	21.6
GPP-Site_B (Scenario 2)	55	738715	4239776	2489	13	17.8	46	9.6	21.6

Meteorological data
The required surface meteorological data for the model, temperature, humidity, precipitation, wind speed and direction and solar radiation were collected by a meteorological station in the Sabalan geothermal field; cloud cover was provided by the Meshkinshahr metrological station, 12 km north of the study area for the period January to August 2009. The upper-air meteorological data were not recorded in the area. Therefore, they were computed by the upper air estimator within AERMET, based on hourly surface meteorological data. Land surface characteristics (albedo, surface roughness, Bowen ratio) for AERMET meteorological pre-processor were set based on the topography and land use in the Sabalan geothermal field.

The predominant winds during the measured time in the NW Sabalan geothermal area blow from the southeast to northwest (Figure 7a) and the main wind speed is 2 ± 1.5 m/s (60%) (Figure 7b).

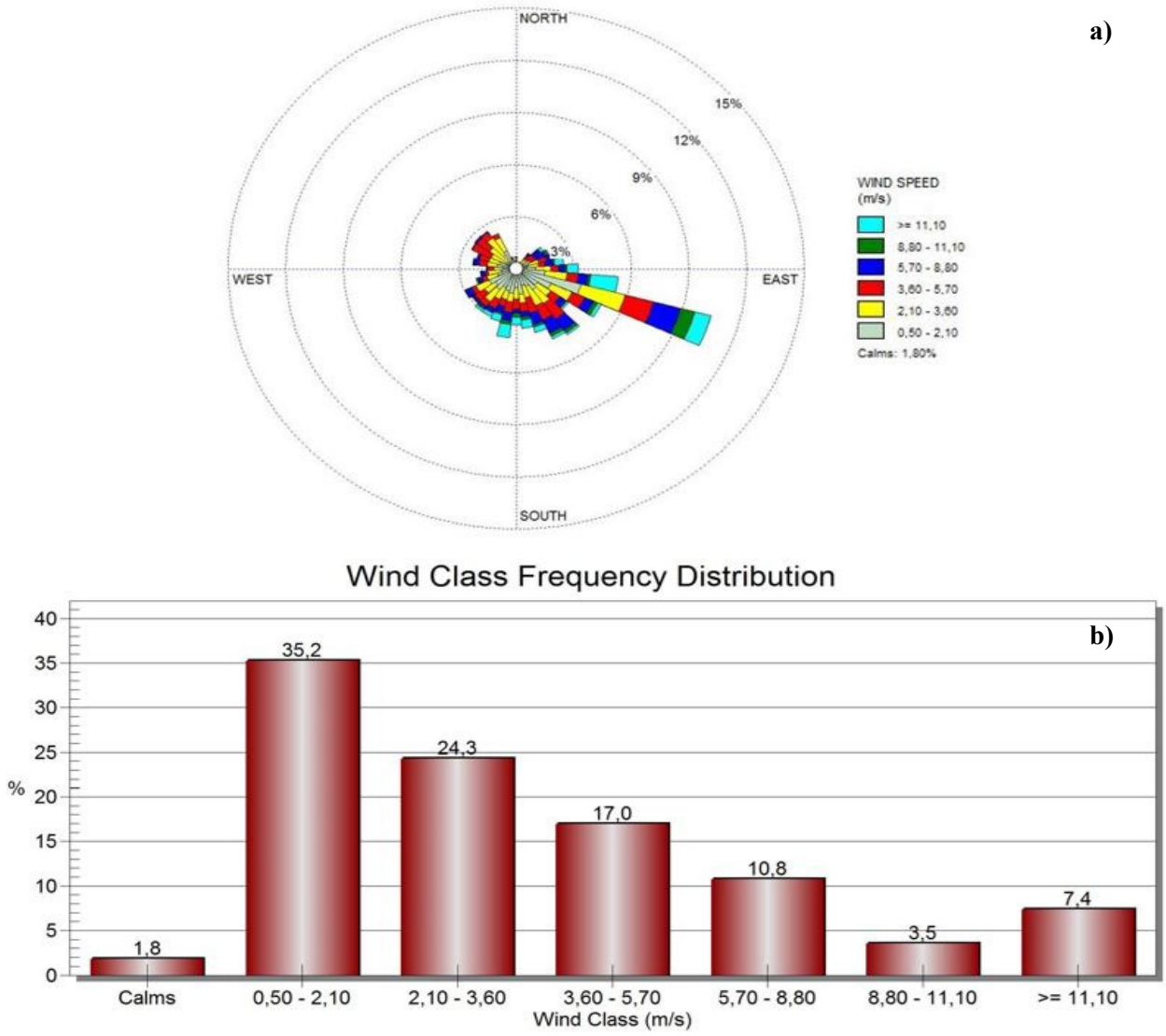

FIGURE 7: Wind rose (a) and wind class frequency distribution (b) in the NW Sabalan weather station January to August in 2009

Terrain data and receptors

There are two basic types of input data that are needed to run the terrain pre-processor (AERMAP). First, AERMAP requires an input file that directs the actions of AERMAP through a set of options, and defines the receptor and source locations. Secondly, AERMAP needs standardized computer files of terrain data and is programmed to read only the USGS format (EPA, 2004).

In this study, the required digital elevation model (DEM) of the study area was downloaded from a USGS website. The DEM file was imported to the terrain pre-processor to calculate the critical dividing streamline height and to determine the hill height scale for each receptor (Figure 8). According to the geographical features of the study area, the flat and elevated option was selected in the model.

For the receptors, considering the populated areas (Moil, Dizo and Valezir villages) near the proposed Sabalan geothermal power plant, discrete Cartesian receptors and uniform Cartesian grids were used in the modelling to determine the area with maximum predicted H_2S concentrations. On the terrain map, the location of the receptor zone was identified using satellite imagery from Google Earth.

With the aim of providing a higher resolution of predicted H_2S concentrations for the area in the vicinity

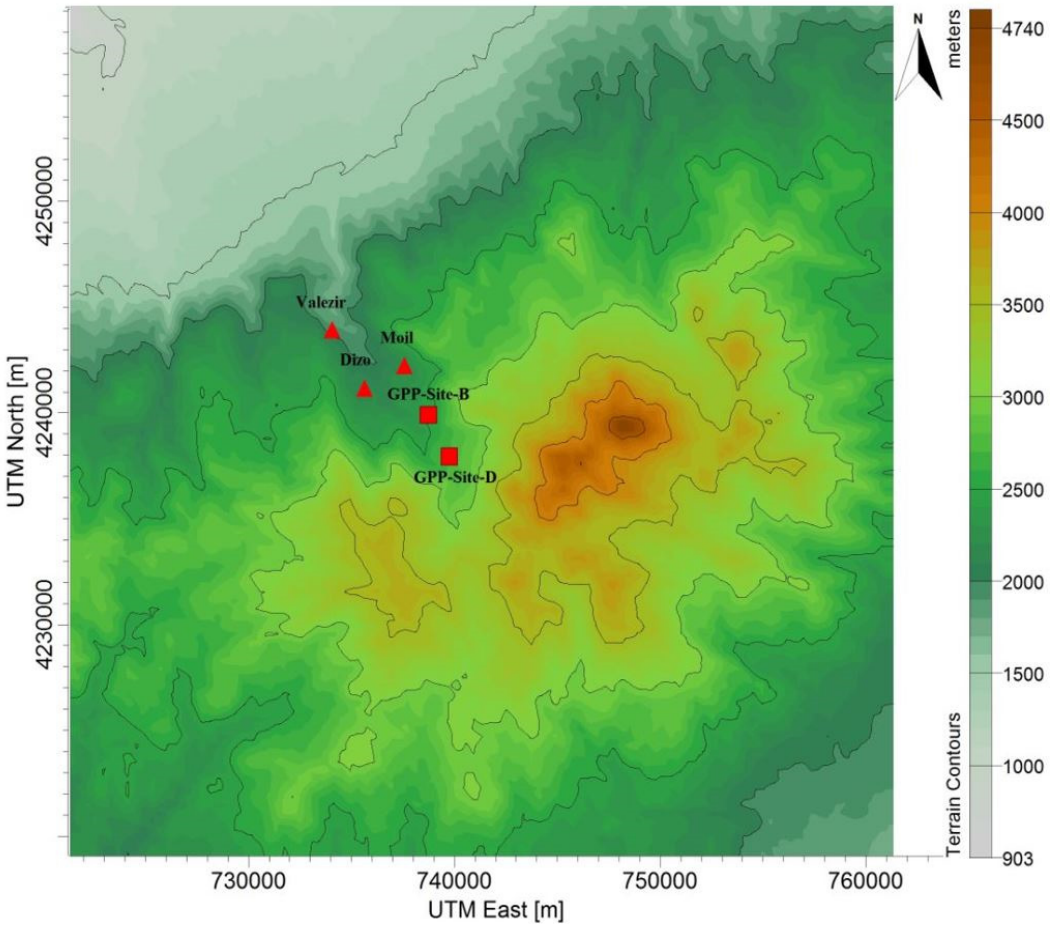

FIGURE 8: The terrain contour map of the study area. Red triangle show locations of populated areas, red squares GPS sites

of the power plant, as well as extending to a broader area from the source, the following grid sizes and resolutions were used together:

- Grid 1 – 39 km × 39 km at 1000 m resolution
- Grid 2 – 15 km × 15 km at 300 m resolution
- Grid 3 – 1.4 km × 1.4 km at 20 m resolution

6. MODELLING RESULTS

After importing all the required data and parameters for running the AREMOD dispersion modelling, the model was finalized to compute the spatial distribution of the plume and H_2S ground level concentrations in the study area.

According to the ambient air quality standards and occupational health guidelines for H_2S for the period average from January to August in 2009, and due to the lack of accurate annual meteorological data, 24, 8 and 1-hour averaging options were chosen to analyse the concentration of H_2S.

The ambient air quality standard for H_2S concentration over 24 hours is 150 $\mu g/m^3$, according to the World Health Organization (WHO), and 50 $\mu g/m^3$, according to the Icelandic air quality guideline. The threshold limit value for H_2S concentration over 8hours is 14000 $\mu g/m^3$, set by the American Conference of Governmental Industrial Hygienists (ACGIH). H_2S air quality standards for 1-hourexposure vary

widely, even in the same country. For instance, in California, it is 42 µg/m^3, in New York 14 µg/m^3, in Arizona 180 µg/m^{3}and, in New Zealand the standard is7 µg/m^3 (Peralta et al., 2013).

6.1 Results for scenario1

The results of the AERMOD modelling for H_2S concentration for the period January to August in 2009 is shown in Figure 9, when the emission source is located at site D. It indicates that the predicted H_2S concentration is very low at the study area. The highest predicted 8 month average H_2S concentration is 2,68µg/m^3, which occurs near the power plant at E739693 m and N4237871 m. Moreover, the Moil, Valezir and Dizo villages, the nearest inhabited areas to the proposed geothermal power plant (GPP), are almost located outside of the plume pathway and the predicted H_2S concentration is about 0.1µg/m^3.

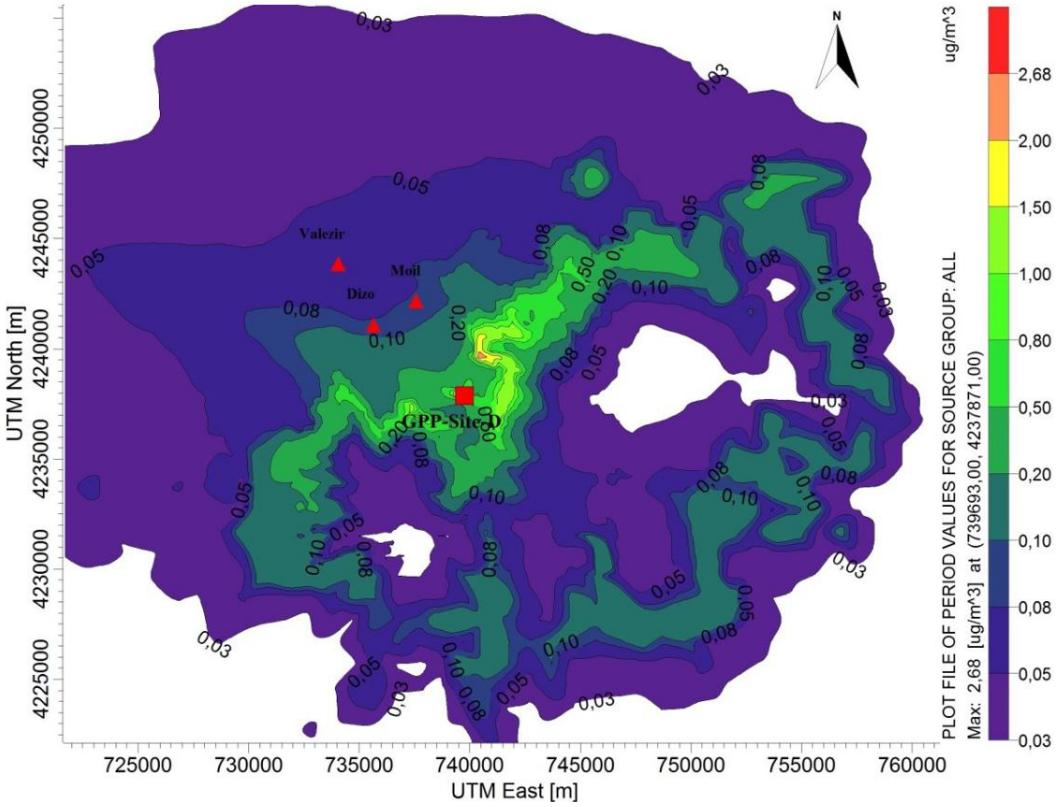

FIGURE 9: Predicted H_2S average concentration for the period January to August in 2009 for scenario 1

The spatial distribution of predicted H_2S concentration for a 24hour averaging time shows that the most common H_2S concentrations in the area are less than 10 µg/m^3 (Figure 10). The maximum levels of H_2S occur north and northwest of the power station, up to 100 µg/m^3, which is in agreement with the predominant winds that blow from the southeast to the northwest. The highest predicted H_2S concentration is 141µg/m^3, 100 m northwest of the power plant.

The dispersion model reveals that for a 24hour averaging period, H_2S concentrations are below the WHO ambient air guideline (150 µg/m^{3}averaged over 24hours), but exceed the Iceland H_2S air ambient standard value (50 µg/m^{3}averaged over 24 hours) in the small area northwest of the source. This area is not considered to have significant impact on public health due to the absence of major human activities.

The AERMOD modelling for an 8-hour averaging time of H_2S concentration (Figure 11) shows that the highest predicted H_2S concentration is 296µg/m^3, northwest of the power plant (Figure 12). TheH_2S concentration is, for the most part, in the range of 5-20 µg/m^3, which is well below the threshold limit value for an 8-hour average concentration, 14000 µg/m^3 (ACGIH).

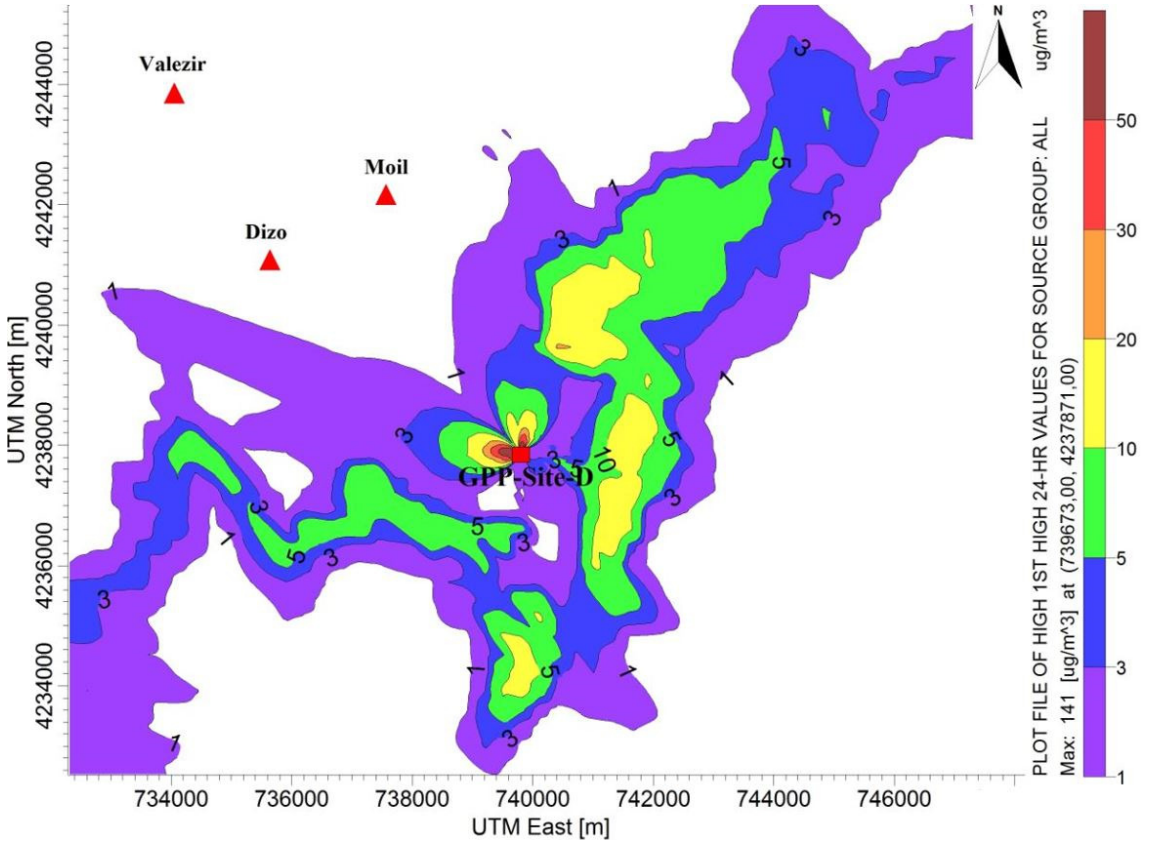

FIGURE 10: Predicted 24-hour average H_2Sconcentrationsfor scenario 1

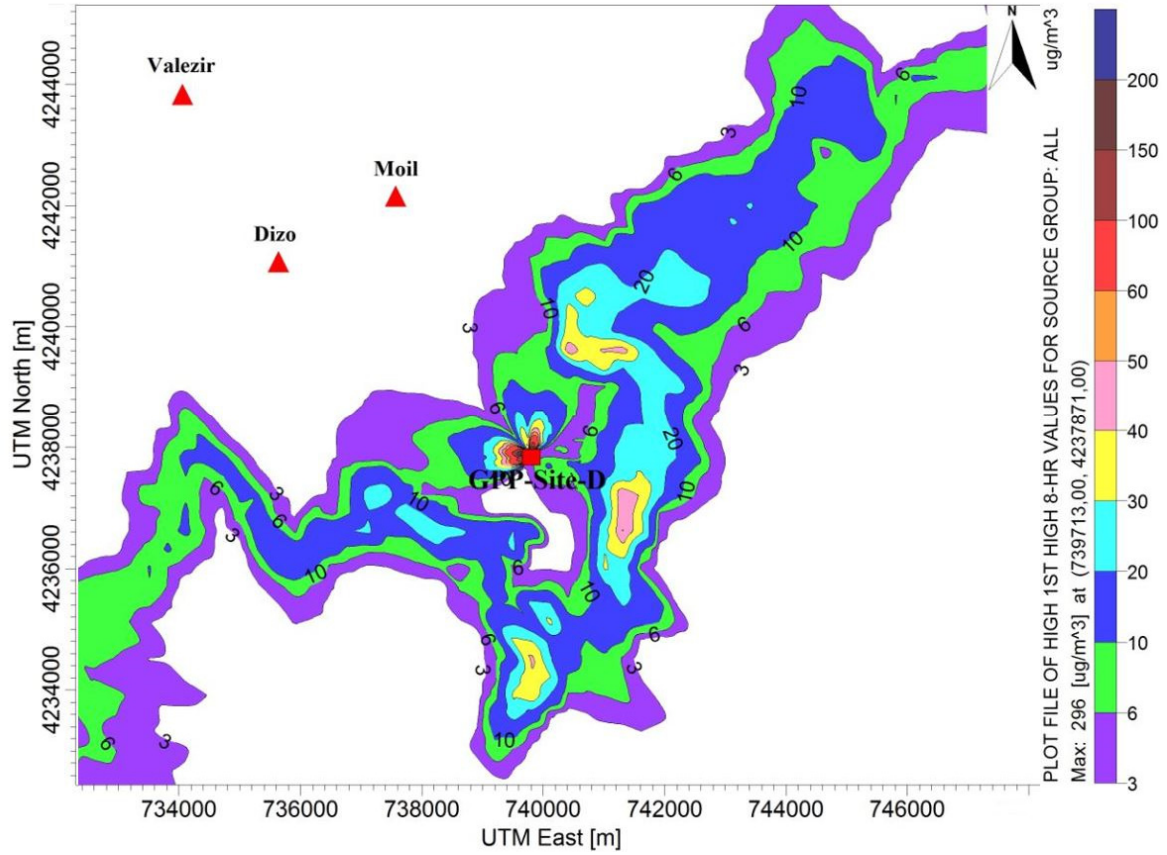

FIGURE 11: Predicted 8hour average H_2S concentrations for scenario 1

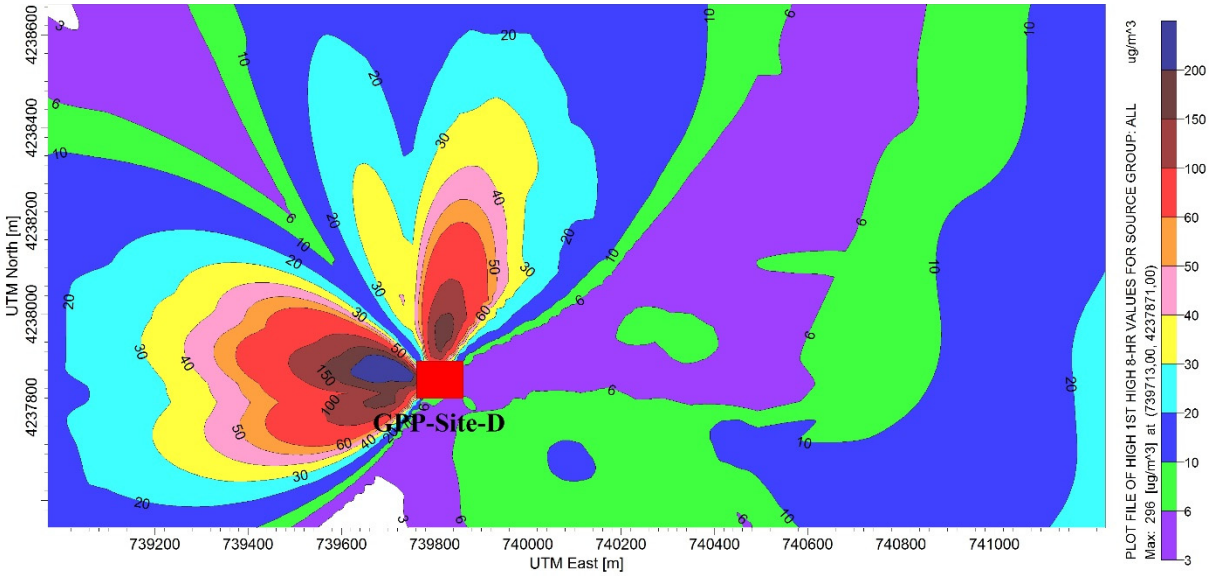

FIGURE 12: Predicted 8 hour average H_2S concentrations emitted close to source for scenario 1

The forecasted maximum H_2S concentrations in an 1hour averaging time indicates that the highestH_2S concentration is 1020 µg/m^3 northwest of the power plant (Figure 13). The maximum level of H_2S for all the computed averaging periods takes place at the same location, on the northwest side of the power plant, in agreement with predominant winds that blow from the southeast to the northwest. This part constitutes a small portion of the study area while for a large part of the area the predicted concentrations range between 10 and 100 µg/m^3. According to the H_2S dispersion pattern in Figure 13, the high levels of the H_2S concentration plume are located east, northeast and southeast of the proposed power plant.

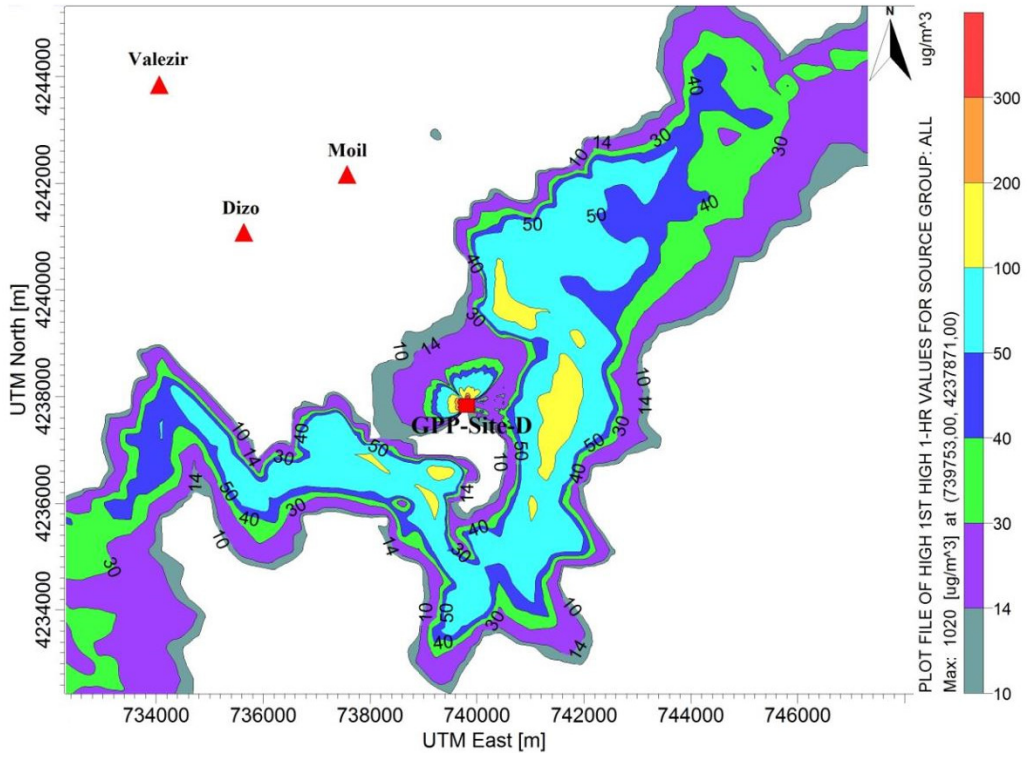

FIGURE 13: Predicted 1-hour average H_2S concentration for scenario 1

In this area, the predicted H_2S concentrations in a 1-hour averaging time are higher than for New Zealand (7 µg/m^3), California (42 µg/m^3) and New York (14 µg/m^3), but less than for Arizona (180 µg/m^3) ambient air quality standards.

6.2 Results for scenario2

The spatial distribution of predicted H_2S concentrations for 1, 8, 24 hours and the averaging time for 8 months from January to August in 2009, were also modelled for scenario 2. The results reveal that there are not many differences between the results of the two scenarios. Therefore, in this part of the report, only the results of the AERMOD modelling for H_2S concentrations for a 24hour averaging period that are important for a health and environmental assessment are shown in Figure 14.

The results indicate that the highest predicted H_2S concentration is equal to 141 µg/m^3, 125 m northwest of the power plant. The most common levels of concentration in the area are less than 10µg/m^3 for a 24-hour averaging time. The simulation shows that the H_2S concentration goes up to 3µg/m^3 in Dizo village, but Moil and Valezir villages are still located outside of the plume pathway. The predicted H_2S concentrations are well below both WHO and Icelandic ambient air standards in the populated area. Therefore, the study suggests that there is no danger to public health and the environment in this area.

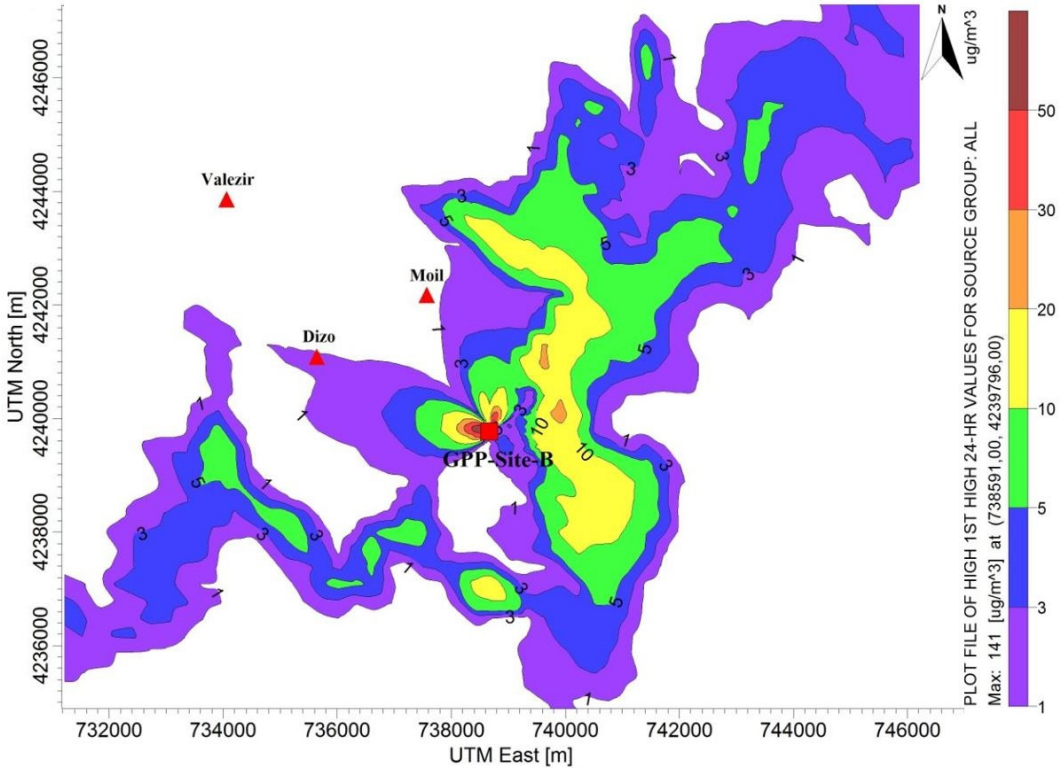

FIGURE 14: Predicted 24-hour average H_2S concentrations for scenario 2

7. CONCLUSIONS

The results of dispersion modelling for scenario 1 indicated that all the populated areas near the planned power plant are located outside the prevailing plume pathway during the modelled period. Furthermore, the dispersion pattern shows that the highest predicted H_2S concentrations for all averaging times occur in the immediate vicinity of the power plant (emission source), in agreement with predominant winds that blow from the southeast to the northwest. The highest predicted H_2S concentrations for the time period: 24hours, 8hours, 1hour, and 8 months are 2.68 µg/m^3, 141 µg/m^3, 296 µg/m^3 and 1020 µg/m^3, respectively.

The plume pathway can reach Dizo village for a 24-hour averaging time in scenario 2, since the emission source is nearby. Nevertheless, the modelled value is less than H_2S air quality standards for a 24-hour averaging time.

The results show that the predicted H_2S concentrations do not exceed the WHO ambient air guideline value for H_2S (150 μg/m^{3}averaged over 24 hours) in either scenario. Whereas, for both scenarios at the limit area close to the source, the predicted H_2S concentrations exceed the Icelandic H_2S air ambient standard value (50 μg/m^{3}averaged over 24 hours).

The occupational exposure limit for H_2S in a workplace, based on the ACGIH occupational safety guideline, is 14000 μg/m^{3}for an 8-hour average and that limit is never exceeded in the study area. However, the predicted H_2S concentration is above the guidelines for New Zealand (7 μg/m^3), California (42 μg/m^3) and New York (14 μg/m^3) but less than for the Arizona (180 μg/m^3) ambient air quality standards for a 1hour average in the large area of northwest Sabalan geothermal field.

The results for both scenarios reveal that spatial distributions of predicted H_2S concentrations follow almost the same pattern, and the difference in location of the Sabalan geothermal power plant in northwest Sabalan geothermal site has no significant effect on the spread of the predicted H_2S plume.

In general, according to the simulation dispersion pattern and the levels of predicted concentrations, the exploitation of the proposed 55 MW Sabalan geothermal power plant does not have a significantly adverse effect on the air quality in the study area. Furthermore, no health impacts are expected for area residents.

Although no environmental and health impacts are anticipated in the study area, dispersion modelling revealed that the large area around the proposed Sabalan geothermal power plant is continuously exposedtoH_2S. Therefore, it is recommended that H_2Sbackground levels and during the operation of the geothermal power plant are monitored continuously in the northwest Sabalan geothermal area in order to assess environmental and health impacts and to suggest mitigating actions if required.

H_2S dispersion modelling is an essential component of environmental and health impact assessment in geothermal areas. It can be used to examine different scenarios, to ensure that the environmental implications of H_2S emission are considered before the decision for construction of a geothermal power plant is taken.

ACKNOWLEDGEMENTS

I would like to express my sincere gratitude to the UNU-GTP for awarding me this scholarship to participate in the six month training programme. I am grateful to my employer, Renewable Energy Organization of Iran and Moshanir Consulting Engineering Company, for giving me this opportunity to undergo geothermal training in Iceland. Best regards are expressed to Mr. Lúdvík S. Georgsson, director of the UNU Geothermal Training Programme, for his hospitality and selfless dedication to the UNU Fellows. Many thanks to Ms. Málfrídur Ómarsdóttir, Ms. Thórhildur Ísberg, Ms. María S. Guðjónsdóttir, Mr. Ingimar Gudni Haraldsson, Mr. Markús A.G. Wilde, and all 2014 UNU fellows for their support, help and the wonderful time we had together during these six months.

I want to give special thanks to my supervisors, Dr. Thröstur Thorsteinsson, Dr. Snjólaug Ólafsdóttir, Dr. Brynhildur Davíðsdóttir and Dr. Matthew J. Roberts, for their dedication, availability, support and guidance while working on this report.

My deepest gratitude goes to my dear wife and my family for their moral and emotional support during these six months. This project is dedicated to my wife, Sepideh Montazer, for her support, and encouragement throughout these six months in Iceland.

REFERENCES

Amistoso, A.E., Buscato, N.M., and Aragon, G.M., 2013*: Discharge testing of NWS6D evaluation report*. Energy Development Corporation, report for SUNA – Renewable Energy Organization of Iran, 25 pp.

Aráuz T., M. A., 2014: *Modeling H_2S Dispersion from San Jacinto Tizate Geothermal Power Plant, Nicaragua.* University of Iceland, Reykjavík, UNU-GTP, MSc thesis, 88 pp.

Bates, M. N., Garrett, N. and Shoemack, P., 2002: Investigation of health effects of hydrogen sulfide from a geothermal source. *Archives of Environmental Health, 57-5*, 405-411.

Bogie, I., Cartwright, A.J., Khosrawi, K., Talebi, B., and Sahabi, F., 2000: The Meshkinshahr geothermal prospect, Iran. *Proceedings of the World Geothermal Congress 2000, Kyushu-Tohoku, Japan*, 997-1002.

Cimorelli, A.J., Perry, S.G.,Venkatram, A., Weil, J.C., Paine, R. J., Wilson, R.B., Lee, R.F., Peters, W.D., Brode, R.W. and Paumier, J.O., 2004: *AERMOD: Description of model formulation.* EPA, report-454/R-03-004, 91 pp. Website: *www.epa.gov/scram001/7thconf/aermod/aermod_mfd.pdf*

DEC, 2005: *Approved methods for the modelling and assessment of air pollutants in New South Wales*. Department of Environment and Conservation, New South Wales, 63 pp. Website: *www.environment.nsw.gov.au/resources/air/ammodelling05361.pdf*

De Kok, L.J., Stuiver, E., Rubinigg, M., Westerman, S., and Grill, D., 1997: Impact of atmospheric sulfur deposition on sulfur metabolism in plants: H_2S as sulfur source for sulfur deprived Brassica Oleracea L. *BotanicaActa*. *110-5*, 411-419.

Durand, M. and Wilson, J.G., 2006: Spatial analysis of respiratory disease on an urbanized geothermal field. *Environmental Research*, *101-2*, 238-245.

EDC, 2007: *A review of NW Sabalan geothermal area resource assessment and development*. Energy Development Corporation, report for SUNA – Renewable Energy Organization of Iran, 61 pp.

EOHP, 2006: *Ambient air guidelines for hydrogen sulphide*. EOHP - Environmental & Occupational Health Program Division of Environmental Health, Maine Center for Disease Control & Prevention, Maine Department of Health & Human Services, 15pp. Website: *www.maine.gov/dep/waste/publications/documents/ambientairguidelines.pdf*

EPA, 2006: *Lesson 6: Plume Dispersion and Air Quality Modelling*. EPA, 18 pp, Website: *yosemite.epa.gov/oaqps/EOGtrain.nsf/fabbfcfe2fc93dac85256afe00483cc4/c9862a32b0eb4f9885256b6d0064ce2b/$FILE/Lesson%206.pdf.*

EPA, 2004: *Users guide For the AERMOD terrain pre-processor (AERMAP).* EPA-454/B-03-003, 106 pp. Website: *www.michigan.gov/documents/deq/deq-aqd-aqe_aermapug_257866_7.pdf*

Faridi, M., 2010: *Structural geology of Mount Sabalan.* SUNA - Renewable Energy Organization of Iran, report, 62 pp.

Franco N., L.A., 2010: Hydrogen sulphide abatement during discharge of geothermal steam from well pads: A case study of well pad TR-18, El Salvador. Report 13 in: *Geothermal training in Iceland 2010*. UNU-GTP, Iceland, 183-212.

Fuller, D.C., and Suruda, A.J., 2000: Occupationally related hydrogen sulfide deaths in the United States from 1984 to 1994. *J. Occup. Med. 42-9,* 939-942.

Gupta, H., and Roy, S., 2007: *Geothermal energy: an alternative resource for the 21st century*. Elsevier B.V., Amsterdam, 279 pp.

Holm, A., Jennejohn, D. and Blodgett, L., 2012: *Geothermal energy and greenhouse gas emissions*. Website: *geo-energy.org/reports/GeothermalGreenhouseEmissionsNov2012GEA_web.pdf,* 14 pp.

Holmes, N.S., and Morawska, L., 2006: A review of dispersion modelling and its application to the dispersion of particles: An overview of different dispersion models available. *Atmospheric Environment*, *40-30*, 5902-5928.

Hung, N.T., 2010: *Urban air quality modelling and management in Hanoi, Vietnam*. National Environmental Research Institute, Aarhus University, Denmark, PhD Thesis, 219 pp. Website: *www2.dmu.dk/pub/phd_hung.pdf.*

Idriss, A., Foster, K.R., Yee, D., Palczynski, R., Dixon, E., Jackson, W. and Kinneburgh, C., 2004: *Assessment report on reduced sulphur compounds for developing ambient air quality objectives*. Report prepared for Alberta Environment, 165 pp. Website: *environment.gov.ab.ca/info/library/6664.pdf.*

Kagel, A., 2008: *The state of geothermal technology, part II: surface technology*. Geothermal Energy Association, publication for the U.S. Department of Energy, 89 pp.

Khalil, M.S., Kord, M., and El-Daly, F.A., 1996: Some enzymatic activities of radish and tomato plants fumigated with a mixture of sulphur dioxide and hydrogen sulphide. *Egyptian J. Physiological Science, 2-1/2,* 81-90.

Kosari T., A., 2011: Interpretation of geochemical well test data for well NWS-6D, NW-Sabalan, Iran: An implication for scaling potential and recommended inhibition methods. Report 18 in: *Geothermal Training in Iceland 2011*. UNU-GTP, Iceland, 357-390.

Kristmannsdóttir, H., Sigurgeirsson, M., Ármannsson, H., Hjartarson, H. and Ólafsson, M., 2000: Sulfur gas emissions from geothermal power plants in Iceland. *Geothermics*, *29-4/5*, 525-538.

Kumar, A., Jampana, S.S., Varadarajan, Ch., 2004: Application of the United States Environmental Protection Agency's AERMOD model to an industrial area. *Environmental Progress*, *23-1*, 12-18.

Macdonald, R., 2003: *Theory and objectives of air dispersion modelling*. University of Waterloo, Waterloo, 27 pp. Website: *www.engga.uwo.ca/people/esavory/MME474A_Part1.pdf.*

McKenzie, D.P., 1972: Active tectonic of Mediterranian region. *Geophys. J. Internat.*, *30*-2, 109-185.

MESB, 2000: *Health effects of low-level hydrogen sulfide in ambient air*. Michigan Environmental Science Board, a science report to Governor John Engler, 43 pp. Accessible at: *www.michigan.gov/documents/h2srept_3700_7.pdf.*

Millachine, M.A., 2011: *Guidelines for optimum gas extraction system selection*. University of Iceland, Reykjavík, MSc thesis, 54 pp.

Neshuku, M.N., 2012: *Comparison of the performance of two atmospheric dispersion models (AERMOD and ADMS) for open pit mining sources of air pollution*. University of Pretoria, MSc thesis, 102 pp.

Nyagah, E.M., 2006: Hydrogen sulphide dispersion and modelling for Nesjavellir power station using Gaussian and numerical models. Report 15 in: *Geothermal Training in Iceland 2006*. UNU-GTP, Iceland, 291-314.

Ólafsdóttir, S., Gardarsson, S.M., Andradóttir, H.O., 2014: Spatial distribution of hydrogen sulfide from two geothermal power plants in complex terrain. *Atmospheric Environment*, *82,* 60-70.

Peralta, O., Castro, T., Durónb, M., Salcido, A., Celada-Murillo, A., Navarro-Gonzálezd, R., Márqueza, C., García, J., Rosa, J., Torres, R., Villegas-Martínez, R., Carreón-Sierra, S., Imaz, M., Martínez-Arroyoa, A., Saavedra, I., Espinosa, M. and Torres-Jaramillo, A., 2013: H_2S emissions from Cerro Prieto geothermal power plant, Mexico, and air pollutants measurements in the area. *Geothermics, 46,* 55–65.

Perry, S.G., Cimorelli, A.J., Paine, R.J., Brode, R.W., Weil, J.C., Venkatram, A., Wilson, R.B., Lee, R. F., and Peters, W.D., 2005: AERMOD: A dispersion model for industrial source applications. Part II: model performance against 17 field study databases. *J. Applied Meteorology, 44-5,* 694-708.

Porkhial, S., Shabihkhani, R., Oladnia, S. and Moridi, A., 2010: Environmental monitoring of air, soil and surface water resources; a case study on Meshkinshahr geothermal field development. *Proceedings of the World Geothermal Congress 2010, Bali, Indonesia,* 7 pp.

Radmehr, B., 2005: Preliminary design of a proposed geothermal power plant in NW-Sabalan area, Iran. Report 15 in: *Geothermal Training in Iceland 2005*. UNU-GTP, Iceland, 265-296.

Renewable Energy Organization of Iran, 2014: *Geothermal energy resources and development in Iran*, SUNA – Renewable Organization of Iran, Deputy for Executive and Technical, Geothermal Energy Office. Website: *www.suna.org.ir/en/executive/geothermalenergy/geothermalen.*

SCOEL, 2007, *Recommendation from the scientific committee on occupational exposure limits for hydrogen sulphide*. SCOEL, 17 pp. Website: *ec.europa.eu/social/BlobServlet?docId=3864&langId=en*

Seangkiatiyuth, K., Surapipith, V., Tantrakarnapa, K. and Lothongkum, A. W., 2011: Application of the AERMOD modelling system for environmental impact assessment of NO_2 emissions from a cement complex. *J. Environmental Sciences, 23-6,* 931–940.

SKM, 2004: *Well NWS-4 discharge evaluation report*. Sinclair Knight Merz, report for SUNA – Renewable Energy Organization of Iran, 27 pp.

SKM, 2005a: *NW-Sabalan geothermal feasibility study*. Sinclair Knight Merz, report for SUNA – Renewable Energy Organization of Iran, 150 pp.

SKM, 2005b: *Geochemical evaluation of well NWS-1 discharge test*. Sinclair Knight Merz, report for SUNA – Renewable Energy Organization of Iran, 24 pp.

Stockie, J.M., 2011: The mathematics of atmospheric dispersion modelling. *SIAM Review*, *53-2,* 349-372. Website: *people.math.sfu.ca/~stockie/atmos/paper.pdf.*

TBCE, 1979: *Geothermal power development studies, Sabalan zone*. TBCE, Geophysical Survey, report to Ministry of Energy, Islamic Republic of Iran.

Vallero, D., 2008: *Fundamentals of air pollution.* Elsevier Inc., Amsterdam, 942 pp. Website: *books.google.is/books?id=4AV2Wds_NZAC&pg=PA581&lpg=PA581&dq#v=onepage&q&f=false.*

Vora, J., 2010: *Dust dispersion modelling for opencast mines*. National Institute of Technology Rourkela, India, BSc thesis, 55 pp. Website: *ethesis.nitrkl.ac.in/1760/1/jinesh.pdf.*

Wahl, E. F., 1977: *Geothermal energy utilization.* John Wiley & Sons, NY, 302 pp.

WHO, 2000: *Hydrogen sulphide*. World Health Organization, regional office for Europe, 7 pp. Website: *www.euro.who.int/__data/assets/pdf_file/0019/123076/AQG2ndEd_6_6Hydrogensulfide.PDF*

WHO, 2003: *Hydrogen sulphide: Human health aspects*. World Health Organization, concise chemical assessment document, 53, 35 pp.

Zou, B., Benjamin Zhan, F., Gaines Wilson, J. and Zeng, Y., 2010: Performance of AERMOD at different time scales. *Simulation Modelling Practice and Theory, 18* 612-623.